ENGINEERING TRANSACTIONS • *Engng. Trans.* • **56**, 4, 363–376, 2008
Polish Academy of Sciences • Institute of Fundamental Technological Research

CONSTITUTIVE MODELLING AND NUMERICAL SIMULATION OF DYNAMIC BEHAVIOUR OF ASPHALT-CONCRETE PAVEMENT

A. Z b i c i a k

Warsaw University of Technology
Faculty of Civil Engineering, Institute of Structural Mechanics
Armii Ludowej 16, 00–637 Warszawa, Poland

The main objective of the paper is to present a simple constitutive model suited for dynamic simulation of asphalt-concrete mixtures. ABAQUS/Explicit FE software is used for this purpose. The model belongs to the class of overstress hypoelastic-viscoplastic materials, taking into account the effect of pressure-dependence on yielding. The implementation of constitutive relations formulated in the paper is done through user subroutine module VUMAT. The results of numerical simulation of dynamic behaviour of multilayer pavement structure, illustrating the applicability of the algorithm, is also discussed.

Key words: dynamic plasticity, asphalt concrete pavement, FEM.

1. Introduction

Rheological properties of engineering materials are characterized by elastic, plastic and viscous phenomena. The plastic behaviour is always associated with large deformations, whereas the viscosity is observed during fast loading. The loads acting on asphalt-concrete pavement structure are dynamic in nature. Thus, the crucial problem in analysis of such pavements is a formulation of constitutive model of the material, taking into account the rate-dependence phenomenon. Our objective is to present a simple class of constitutive equations describing the behaviour of pressure-sensitive materials such as asphalt concrete, suited for dynamic simulation. During our investigation we will not consider any creep effects because the analysis is limited to fast loading processes [2, 19].

Within the framework of the theory of viscoplasticity [16] it is possible to consider the influence of load intensity as well as its velocity on the process of formation of permanent deformations. The theory states that there is a limit state of stress defining the range of elastic behaviour. We assume that the limit state may be defined by the yield function depending on two invariants – the norm of deviatoric stress and the trace of the stress tensor. After reaching the limit state, viscoplastic effects may be observed. In order to describe the viscosity phenomenon, additional parameters should be taken into consideration.

The model presented herein introduces only one viscous parameter related to the total stress space. Thus, the relations to be obtained belongs to the class of Duvaut-Lions overstress materials [6] in which the rate-independent plastic part of the stress tensor may be calculated as a projection of the total stress on the static yield surface.

We will start with large strain formulation. After some simplifying assumptions, a hypoelastic-viscoplastic model will be introduced. The form of constitutive relationships to be obtained herein allows a user-defined implementation within the Finite Element (FE) commercial codes. The numerical integration algorithm was coded in ABAQUS software [1]. The implementation was done through user subroutine module VUMAT in order to study the behaviour of multilayer pavement structure.

2. Kinematics

Analysing large elasto-viscoplastic deformations we should start with an assumption stating that the total deformation gradient $\mathbf{F}$ is decomposed multiplicatively into elastic and viscoplastic parts [11, 12]

$$\mathbf{F} = \mathbf{F}^e\,\mathbf{F}^{vp}, \qquad \text{if} \qquad d\mathbf{x} = \mathbf{F}\,d\mathbf{X}, \tag{2.1}$$

where $\mathbf{F}$ maps a line element $d\mathbf{X}$ in the reference configuration to the $d\mathbf{x}$ in the deformed configuration.

In Eq. (2.1), both tensors $\mathbf{F}^e$ as well as $\mathbf{F}^{vp}$ contain stretches and rigid body rotations. For simplification we will assume that all rigid rotations are associated with viscoplastic deformation gradient. Thus, using the polar decomposition theorem we obtain

$$\mathbf{F}^e = \mathbf{V}^e \qquad \text{and} \qquad \mathbf{F}^{vp} = \mathbf{V}^{vp}\mathbf{R}, \tag{2.2}$$

where $\mathbf{R}$ describes total rotations. Moreover, $\mathbf{V}^e$ and $\mathbf{V}^{vp}$ are left stretch tensors in elastic and viscoplastic part respectively.

Differentiating Eq. $(2.1)_2$ and making use of Eq. $(2.1)_1$, we obtain the following expression defining velocity gradient $\mathbf{L}$ as well as its elastic and viscoplastic parts given by $\mathbf{L}^e$ and $\mathbf{L}^{vp}$:

$$\mathbf{L} = \frac{d\,\mathbf{v}}{d\,\mathbf{x}} = \dot{\mathbf{F}}\,\mathbf{F}^{-1} = \mathbf{L}^e + \mathbf{V}^e\mathbf{L}^{vp}\,(\mathbf{V}^e)^{-1} \tag{2.3}$$

$$\text{if} \quad \mathbf{L}^e = \dot{\mathbf{V}}^e\,(\mathbf{V}^e)^{-1} \quad \text{and} \quad \mathbf{L}^{vp} = \dot{\mathbf{F}}^{vp}\,(\mathbf{F}^{vp})^{-1}.$$

The velocity gradient can be decomposed into a symmetric part denoted by $\mathbf{D}$ and a skew-symmetric part denoted by $\mathbf{W}$

$$\mathbf{L} = \mathbf{D} + \mathbf{W} \quad \text{where} \quad \mathbf{D} = \frac{1}{2}\left(\mathbf{L} + \mathbf{L}^T\right) \quad \text{and} \quad \mathbf{W} = \frac{1}{2}\left(\mathbf{L} - \mathbf{L}^T\right). \tag{2.4}$$

Of course, the same decomposition scheme holds for its elastic part $\mathbf{L}^e = \mathbf{D}^e + \mathbf{W}^e$ and viscoplastic part $\mathbf{L}^{vp} = \mathbf{D}^{vp} + \mathbf{W}^{vp}$. Thus, based on Eq. $(2.3)_1$ we obtain

$$\mathbf{L} = \mathbf{D}^e + \mathbf{W}^e + \mathbf{V}^e\mathbf{D}^{vp}\,(\mathbf{V}^e)^{-1} + \mathbf{V}^e\mathbf{W}^{vp}\,(\mathbf{V}^e)^{-1}\,. \tag{2.5}$$

Eventually, taking the symmetric part in Eq. (2.5) we obtain

$$\mathbf{D} = \text{sym}\ (\mathbf{L}) = \mathbf{D}^e + \text{sym}\left[\mathbf{V}^e\mathbf{D}^{vp}\,(\mathbf{V}^e)^{-1}\right] + \text{sym}\left[\mathbf{V}^e\mathbf{W}^{vp}\,(\mathbf{V}^e)^{-1}\right]. \tag{2.6}$$

Assuming that elastic stretches are small, i.e. $\mathbf{V}^e = (\mathbf{V}^e)^{-1} = \mathbf{I}$, we obtain from (2.6) the well-known decomposition rule for the rate of deformation tensor

$$\mathbf{D} = \mathbf{D}^e + \mathbf{D}^{vp}. \tag{2.7}$$

The decomposition scheme expressed by Eq. (2.7), along with assumption stating that $\mathbf{W}^{vp} = \mathbf{0}$, is widely used in FEM programmes [3, 18].

3. Constitutive relationships

We assume that the elastic part is described by hypoelastic law relating any objective rate of Kirchhoff stress $\boldsymbol{\tau}^{\nabla}$ to the elastic rate of deformation

$$\boldsymbol{\tau}^{\nabla} = \mathsf{C} \cdot \mathbf{D}^e, \tag{3.1}$$

where the C denotes the 4th rank tensor of elastic coefficients.

Combining Eq. (2.7) with Eq. (3.1) we obtain

$$\boldsymbol{\tau}^{\nabla} = \mathsf{C} \cdot (\mathbf{D} - \mathbf{D}^{vp})\,. \tag{3.2}$$

In the case of isotropy, the above equation is replaced by

$$\boldsymbol{\tau}^{\nabla} = K\ \text{tr}\,(\mathbf{D} - \mathbf{D}^{vp})\ \mathbf{I} + 2\,G\ \text{dev}\,(\mathbf{D} - \mathbf{D}^{vp})\,, \tag{3.3}$$

where the elastic constants K and G denote the bulk modulus and shear modulus respectively.

The operators $\text{tr}\,(\cdot)$ and $\text{dev}\,(\cdot) := (\cdot) - \dfrac{1}{3}\,\text{tr}\,(\cdot)\,\mathbf{I}$ used in Eq. (3.3) denote the trace and deviator.

The objective rate of the tensor $\boldsymbol{\tau}$ in the above expressions is given by

$$\boldsymbol{\tau}^{\nabla} = \dot{\boldsymbol{\tau}} + \boldsymbol{\tau}\,\boldsymbol{\Omega} - \boldsymbol{\Omega}\,\boldsymbol{\tau}, \tag{3.4}$$

where $\dot{\boldsymbol{\tau}}$ is the material rate with respect to the basis of $\boldsymbol{\tau}$. The $\boldsymbol{\Omega}$ is a skew-symmetric spin tensor. Various forms of $\boldsymbol{\Omega}$ can be taken into account. For example setting $\boldsymbol{\Omega} = \mathbf{W}$ in Eq. (3.4), gives the Jaumann rate. Another objective stress

rate, the Green–Naghdi rate, is obtained by taking $\mathbf{\Omega} = \dot{\mathbf{R}}\,\mathbf{R}^T$. For numerical simulations, the Green–Naghdi rate will be used because of needs of the user material subroutine implemented in FE code.

The additive decomposition of the rate of deformation tensor introduced in Eq. (2.7), may be interpreted via rheological model to be shown in Fig. 1. Such a model, firstly defined by Bingham in the case of 1D stress-strain state, represents a family of elasto-viscoplastic materials called over-stress type models [12]. For such materials, before reaching a plastic limit state, the material behaves like a perfectly elastic one. After that, a rate-dependent yielding is observed.

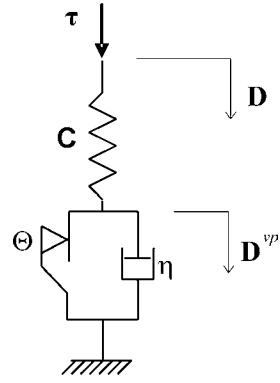

FIG. 1. Rheological model of the material.

Based on the Fig. 1, it can be proved that the total stress $\boldsymbol{\tau}$ is equal to elastic stress $\boldsymbol{\tau}^e$ and may be decomposed into the stress acting in plastic network $\boldsymbol{\tau}^p$ and viscous network $\boldsymbol{\tau}^v$. Thus, we have the relation

$$\boldsymbol{\tau} = \boldsymbol{\tau}^e = \boldsymbol{\tau}^p + \eta\,\mathbf{D}^{vp}, \tag{3.5}$$

in which scalar η denotes the viscosity parameter. This is the only rate-dependent material coefficient to be taken into consideration. In general case, one should consider a tensor of viscous parameters being similar to the elastic operator C or assume two coefficients related to volumetric and deviatoric subspaces like in Eq. (3.3). Because of the complexity of laboratory tests for asphalt, we assume only the single-rate-parameter model.

Now we need to describe the plastic properties of our model. The system of constitutive relations of a perfectly plastic material is defined by the set of admissible stresses Θ as well as by the maximum dissipation rule [15]:

$$\boldsymbol{\tau}^p \in \Theta, \tag{3.6}$$

$$\mathbf{D}^{vp} \in \mathcal{K}\,(\boldsymbol{\tau}^p,\,\Theta) := \{\boldsymbol{\tau}^p\colon \mathbf{D}^{vp}\cdot(\boldsymbol{\tau}^p - \tilde{\boldsymbol{\tau}}) \geq 0 \quad \forall\,\tilde{\boldsymbol{\tau}} \in \Theta\}\,. \tag{3.7}$$

It should be assumed that the Θ-set is convex, closed, limited and contains zero. The mapping $\mathcal{K}$ used in Eq. (3.7), determines the set of viscoelastic rates assigned to $\boldsymbol{\tau}^p$. This set has the form of an external normal cone to the Θ-set at $\boldsymbol{\tau}^p$.

Alternatively, the system of Eqs. (3.5), (3.6) and (3.7), may be replaced by the following minimization problem:

$$\mathbf{D}^{vp} = \arg\min_{\widetilde{\mathbf{D}}} \left[\frac{1}{2}\eta \left\|\widetilde{\mathbf{D}}\right\|^2 + \Pi_\Theta\left(\widetilde{\mathbf{D}}\right) - \boldsymbol{\tau}\cdot\widetilde{\mathbf{D}}\right] \tag{3.8}$$

$$\text{if} \qquad \Pi_\Theta\left(\widetilde{\mathbf{D}}\right) := \sup_{\boldsymbol{\tau}^p\in\Theta} \widetilde{\mathbf{D}}\cdot\boldsymbol{\tau}^p,$$

where Π_Θ denotes the support functional of the Θ-set [15].

The system of constitutive relations given by Eqs. (3.3), (3.5), (3.6) and (3.7) or by Eqs. (3.3) and (3.8) is valid for any isotropic elasto-viscoplastic material in which the plasticity constraints are described by appropriate definition of the Θ-set. Let us assume that this set is described by smooth yield function Φ as follows:

$$\Theta := \left\{\boldsymbol{\tau}^p \colon \Phi\left(\boldsymbol{\tau}^p\right) \le 0\right\}. \tag{3.9}$$

Thus, we can replace the Eqs. (3.6) and (3.7) by the following set [8]:

$$\mathbf{D}^{vp} = \lambda\frac{\partial\Phi\left(\boldsymbol{\tau}^p\right)}{\partial\boldsymbol{\tau}^p}, \qquad \Phi\left(\boldsymbol{\tau}^p\right) \le 0, \qquad \lambda \ge 0, \qquad \lambda\Phi\left(\boldsymbol{\tau}^p\right) = 0, \tag{3.10}$$

where the scalar λ is called the Lagrange multiplier. Equation $(3.10)_1$ is called the associated flow rule while Eqs. $(3.10)_2$, $(3.10)_3$ and $(3.10)_4$ are the loading/unloading conditions or Kuhn–Tucker conditions.

Obtaining of the detailed form of Eqs. (3.10) needs the appropriate yield condition to be taken into consideration. In the paper we will analyse a pressure-sensitive Mises–Schleicher (MS) yield condition [5]. The yield function associated with this condition has a form

$$\Phi\left(\boldsymbol{\tau}^p\right) = \|\text{dev }\boldsymbol{\tau}^p\|^n + \alpha R^{n-1}\,\text{tr}\,\boldsymbol{\tau}^p - R^n \qquad \text{where} \qquad R = \sqrt{2}\,k. \tag{3.11}$$

Three additional material parameters were introduced via Eq. (3.11). Symbol k denotes the yield limit stress based on pure shear test. Dimensionless parameters $\alpha \ge 0$ and $n \ge 1$ determine the shape of the yield function in the meridian cross-section visualized in Fig. 2a.

Taking $\alpha = 0$ and $n = 2$ in Eq. (3.11) we obtain the pressure-insensitive Huber–Mises–Hencky (HMH) yield condition. If we substitute $n = 1$ in Eq. (3.11), we will obtain the Drucker–Prager (DP) yield function. Let us note that the DP

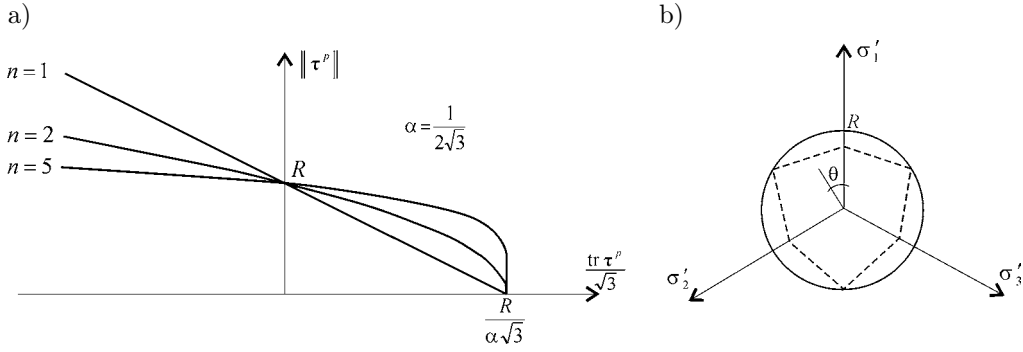

FIG. 2. Meridian (a) and deviatoric (b) sections of the Mises-Schleicher yield surface.

function is non-differentiable for $\operatorname{tr}\boldsymbol{\tau}^p = R/\alpha$. In this point the Eqs. (3.10) are not valid. The analysis of non-smooth yield surfaces is still an open problem in the theory of plasticity. This is not our objective to deal with this problem, so our formulation will be limited to this specific point.

Deviatoric section of MS yield function is of circular shape as it is shown in Fig. 2b (continuous line). In this figure we visualized also, by a dashed line, the locus of Coulomb–Mohr (CM) yield function to be widely used in geomechanics [5]. The CM yield condition may be defined by the following equation:

$$\frac{\operatorname{tr}\boldsymbol{\tau}^p}{3}\sin\phi + \frac{1}{\sqrt{2}}\|\boldsymbol{\tau}^p\|\left[\sin\Big(\theta+\frac{\pi}{3}\Big)+\frac{1}{\sqrt{3}}\cos\Big(\theta+\frac{\pi}{3}\Big)\sin\phi\right] - c\,\cos\,\phi = 0, \tag{3.12}$$

$$\text{for} \qquad \theta \in \langle 0,\, \pi/3\rangle \qquad \text{where} \qquad \theta = \frac{1}{3}\arccos\frac{\sqrt{6}\,\operatorname{tr}\,(\boldsymbol{\tau}^p)^3}{\|\boldsymbol{\tau}^p\|^3}.$$

The CM yield condition defines a yield function having the shape of a pyramid with non-regular hexagonal base. The material parameters k and α describing the MS function, can be evaluated based on the CM coefficients: ϕ – friction angle and c – cohesion parameter. Assuming that the CM surface is inscribed in the DP surface and that their apexes coincide, the following relations between the material coefficients of both conditions are valid:

$$k = \frac{6\cos\phi}{\sqrt{3}\,(3-\sin\phi)}c, \qquad \alpha = \frac{2\sqrt{2}\sin\phi}{\sqrt{3}\,(3-\sin\phi)}. \tag{3.13}$$

Having assumed the MS yield condition, we can specify the relation $(3.10)_1$

$$\mathbf{D}^{vp} = \lambda n\,\|\operatorname{dev}\boldsymbol{\tau}^p\|^{n-2}\operatorname{dev}\boldsymbol{\tau}^p + \lambda\alpha R^{n-1}\mathbf{I}. \tag{3.14}$$

The system of relationships defining our material model is composed of Eqs. (3.3), (3.5), (3.11) and (3.14) completed by conditions $(3.10)_2$, $(3.10)_3$

and $(3.10)_4$. Using these relations we need to have the λ multiplier calculated. After this we can calculate the rate of viscoplastic deformation from Eq. (3.14) and substitute it into Eq. (3.3) in order to obtain the objective stress rate $\boldsymbol{\tau}^{\nabla}$. Finally, using Eq. (3.4) the material stress rate $\dot{\boldsymbol{\tau}}$ may be calculated.

Numerical simulations of the pavement structure will be carried out using the explicit integration algorithm implemented in ABAQUS software (the equations of motion will be solved explicitly). The incremental steps needed for dynamic explicit codes are very small. Thus, we can use the following simple explicit integration scheme in order to update the stress tensor:

$$\boldsymbol{\tau}_{t+\Delta t} = \boldsymbol{\tau}_t + \dot{\boldsymbol{\tau}}\,\Delta t. \tag{3.15}$$

In order to obtain the Lagrange multiplier, we have to analyse two cases. If $\Phi(\boldsymbol{\tau}) \leq 0$, then $\lambda = 0$ and $\mathbf{D}^{vp} = \mathbf{0}$ and $\boldsymbol{\tau}^p = \boldsymbol{\tau}^e = \boldsymbol{\tau}$ (elastic case). If $\Phi(\boldsymbol{\tau}) > 0$, then $\Phi(\boldsymbol{\tau}^p) = 0$ and $\lambda > 0$. In this case the value of λ can be obtained based on Eqs. (3.5), (3.11) and (3.14). We may rewrite these equations eliminating $\mathbf{D}^{vp}$, what gives the following two relations:

$$\boldsymbol{\tau} = \boldsymbol{\tau}^p + \lambda\eta n \left\|\operatorname{dev}\boldsymbol{\tau}^p\right\|^{n-2} \operatorname{dev}\boldsymbol{\tau}^p + \lambda\eta\alpha R^{n-1}\mathbf{I}, \tag{3.16}$$

$$\left\|\operatorname{dev}\boldsymbol{\tau}^p\right\|^n + \alpha R^{n-1}\operatorname{tr}\boldsymbol{\tau}^p - R^n = 0. \tag{3.17}$$

After some algebra, these equations may be written as follows:

$$\lambda = \frac{\|\operatorname{dev}\boldsymbol{\tau}\| - \|\operatorname{dev}\boldsymbol{\tau}^p\|}{n\eta\left\|\operatorname{dev}\boldsymbol{\tau}^p\right\|^{n-1}}, \tag{3.18}$$

$$\left\|\operatorname{dev}\boldsymbol{\tau}^p\right\|^n + \alpha R^{n-1}\left(\operatorname{tr}\boldsymbol{\tau} - 3\lambda\eta\alpha R^{n-1}\right) - R^n = 0. \tag{3.19}$$

In the above scalar equations, the unknowns are λ and $\|\operatorname{dev}\boldsymbol{\tau}^p\|$. It is obvious that for any $n > 1$ and $\alpha \neq 0$, we cannot give any explicit formula for the λ multiplier. In such a case we have to solve the nonlinear algebraic Eq. (3.19). For numerical simulations to be shown in the next chapter, the implicit Newton method was used.

Let us take into consideration two special cases in which the multiplier λ can be expressed in explicit form. For the DP yield function we take $n = 1$. Thus, it can be proved that

$$\lambda = \frac{\|\operatorname{dev}\boldsymbol{\tau}\| + \alpha\operatorname{tr}\boldsymbol{\tau} - R}{\eta\left(1 + 3\alpha^2\right)} \qquad \text{and} \qquad \mathbf{D}^{vp} = \lambda\left(\frac{\operatorname{dev}\boldsymbol{\tau}}{\|\operatorname{dev}\boldsymbol{\tau}\|} + \alpha\mathbf{I}\right). \tag{3.20}$$

In the case of the HMH yield condition, substituting $\alpha = 0$ into Eq. (3.20) we obtain a well-known formula (see [4])

$$\mathbf{D}^{vp} = \frac{\operatorname{dev}\boldsymbol{\tau}}{\eta}\left(1 - \frac{R}{\|\operatorname{dev}\boldsymbol{\tau}\|}\right). \tag{3.21}$$

It is obvious that for the HMH yield criterion, the plastic deformation does not cause any volume changes. Thus, the Eq. (3.21) may be rewritten replacing the Kirchhoff stress tensor $\boldsymbol{\tau}$ by the Cauchy stress tensor $\boldsymbol{\sigma}$.

4. Application

The aim of formulation of constitutive equations is to predict the behaviour of pavement structure under dynamic load. The problem we should solve is a coupled system composed of initial-boundary-value problem, given by the momentum equilibrium and the constitutive equations. Since the boundary-value problem is usually solved by the FEM, the constitutive model has to be implemented in an appropriate way.

The constitutive equations considered can be mathematically classified as a coupled system of non-linear ordinary differential equations, building an initial-value problem. The solution of such a system can be embedded in an incremental FEM formulation with displacement approach, leading to the well-known explicit FEM problem for non-linear material equations, which has to be solved iteratively [3]. The constitutive equations were programmed within the ABAQUS/Explicit system [1]. The system requires the incremental procedure to be defined in VUMAT subroutine coded in FORTRAN language.

In this section we will show the results of dynamic simulation of multilayer asphalt concrete pavement exposed to the impulse of pressure. Such a load may be a simplified model of the aircraft tire impact at the time of landing [13, 14]. We will assume the axisymmetric topology of the model. The schematic view of the model is visualized in Fig. 3. The load acts during 0.1 [s] with the intensity of $q = 1200$ [kPa]. The pressure is uniformly distributed over the circular area with the radius equal to 20 [cm]. The pavement layers were modelled using 2820 axisymmetric 4-node elements of the CAX4 type (see [1]). They rest on a discrete Kelvin–Voigt viscoelastic foundation have the elasticity parameter equal to $\overline{k} = 150$ [MN/m^3] and the viscosity module $\overline{\eta} = 1$ [MNs/m^3]. The FE mesh is built over the 1.4 [m]×4.0 [m] rectangular area.

We carried out three numerical calculations assuming various material properties of the pavement layers. The first simulation was executed for a perfectly-elastic material. The values of elastic parameters (see Table 1) are assumed to be partially based on [10, 19] and are of the same value like in [20]. The parameters presented in Table 1 were also used for next simulations.

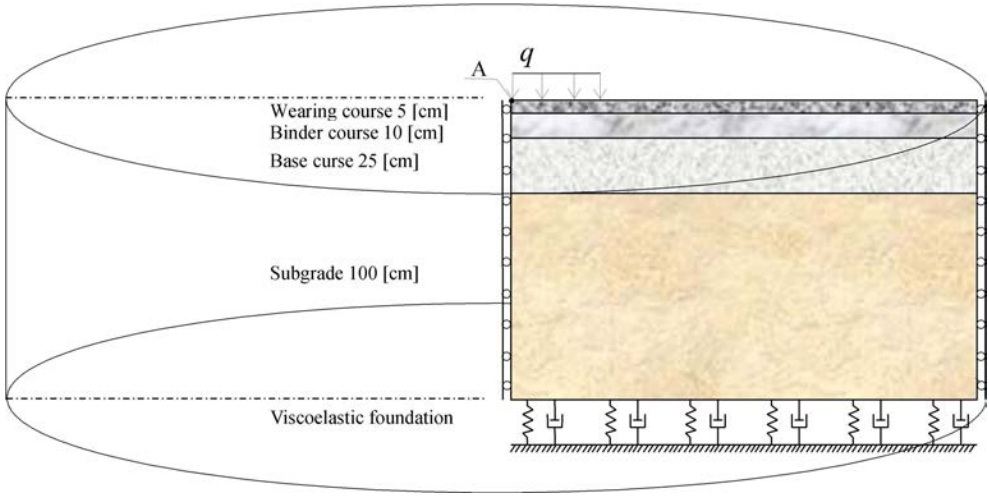

FIG. 3. Schematic view of the structure.

Table 1. Elastic parameters of pavement layers.

	K [MPa]	G [MPa]
Wearing course	160	74
Binder course	186	86
Base course	439	203
Subgrade	125	58

The second simulation was carried out for elasto-plastic rate-independent material with MS yield condition. The inelastic material constants for each layer have the following values: $n = 1.2$; $k = 160$ [kPa] and $\alpha = 0.2$.

The third simulation concerns the elastic-viscoplastic model presented in the previous section. The material constants are of the same value like in previous simulation with the additional viscosity parameter equal to $\eta = 500$ [kPa $\cdot$ s].

The contours of equivalent HMH stress are visualized in Figs. 4 and 5 (elasto-plastic pavement) and in Figs. 6 and 7 (elasto-viscoplastic pavement). The scale deformation factor to be used in these figures is equal to 20. The contour plots show differences in distributions of stresses at the moment of unloading for $t = 0.1$ [s], as well as at the end of analysis for $t = 1$ [s].

Additionally, Fig. 8 shows the displacement history curves at point A located in wearing course (see Fig. 3), constructed for three material models to be taken into consideration. The results allow to evaluate both the maximum deflection and the maximum permanent deflection in the structure. Thus, the maximum deflections to be obtained have the values between approx. 2 [mm] (elastic pavement) and approx. 4.5 [mm] (elasto-plastic pavement). When the load is

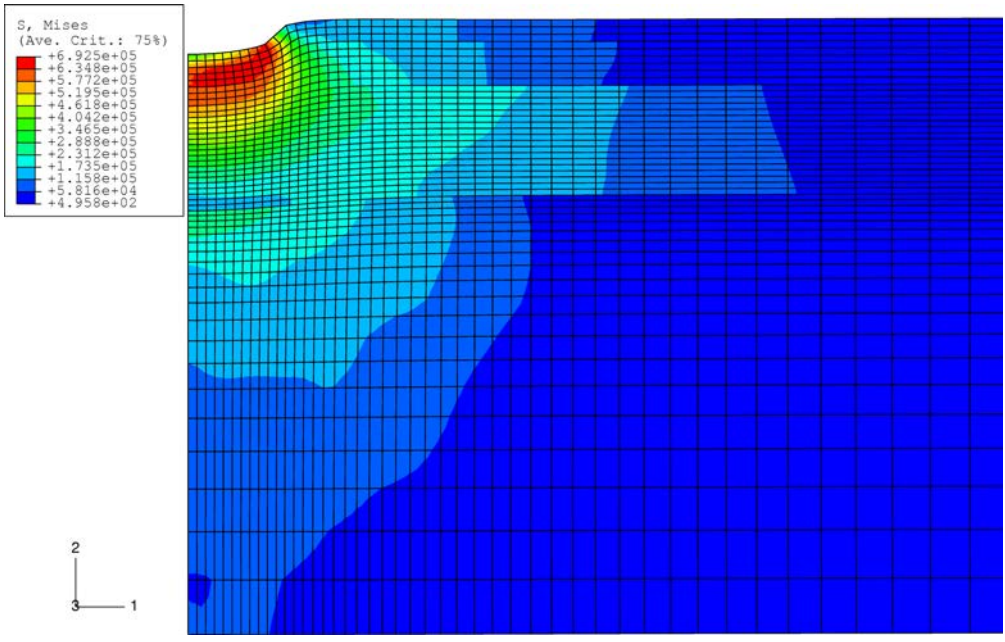

FIG. 4. Contours of equivalent HMH stress in elasto-plastic pavement for $t = 0.1$ [s].

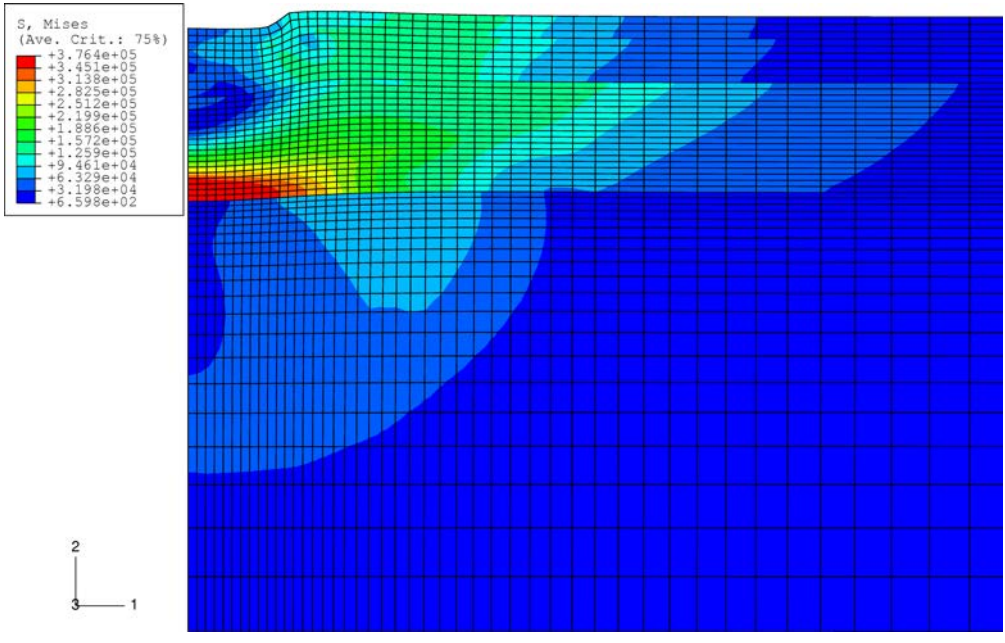

FIG. 5. Contours of equivalent HMH stress in elasto-plastic pavement for $t = 1$ [s].

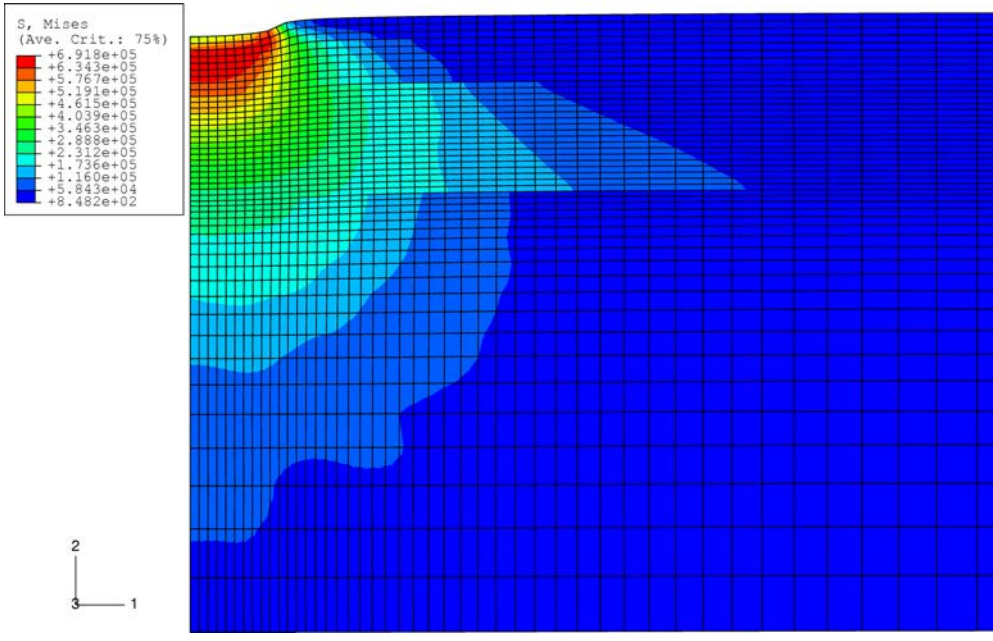

FIG. 6. Contours of equivalent HMH stress in elasto-viscoplastic pavement for $t = 0.1$ [s].

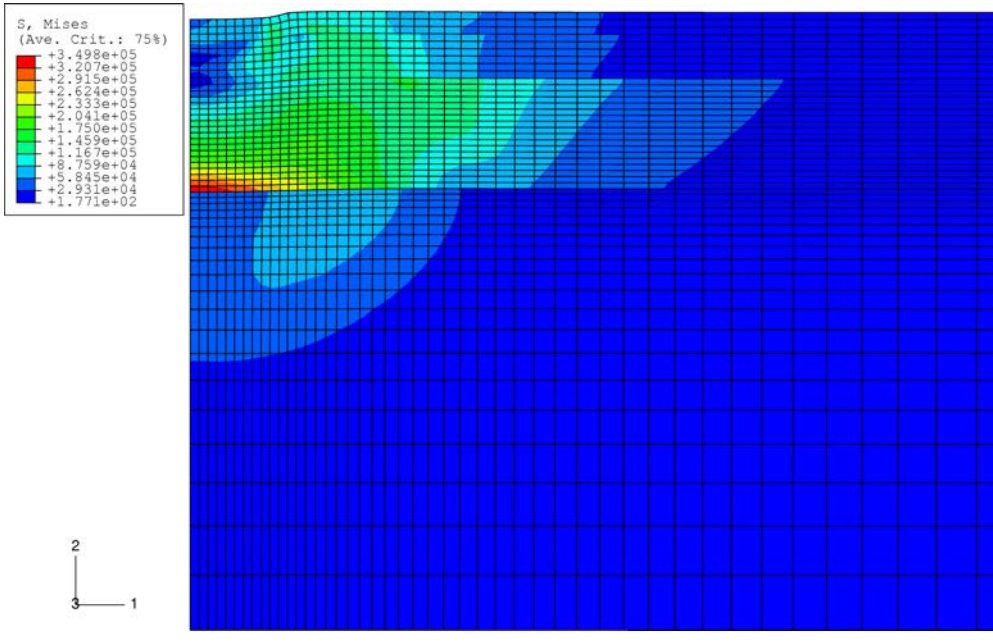

FIG. 7. Contours of equivalent HMH stress in elasto-viscoplastic pavement for $t = 1$ [s].

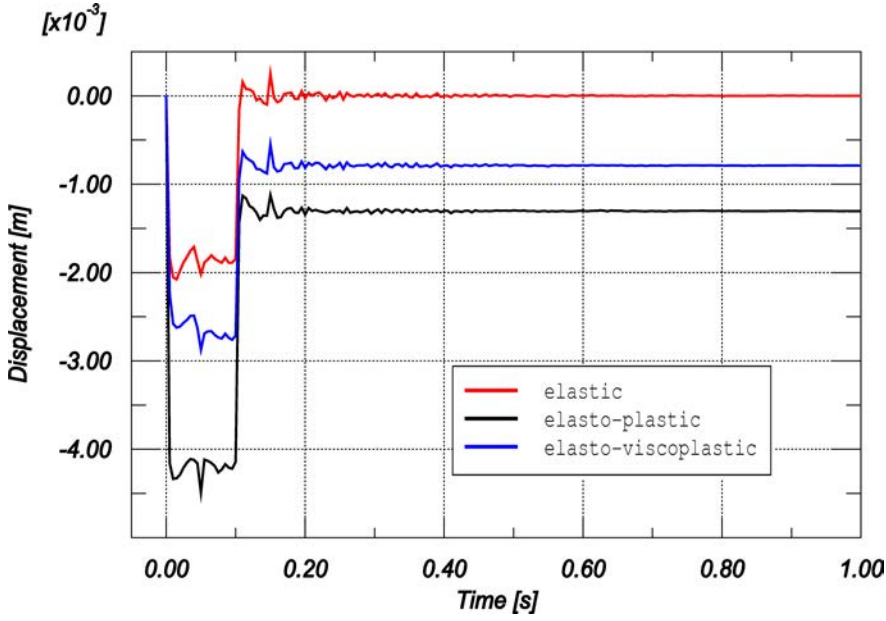

FIG. 8. Vertical displacement history curves for various materials of the pavement structure.

removed, the permanent vertical displacements are equal to approx. 1.3 [mm] (elasto-plastic pavement) and approx. 0.8 [mm] (elasto-viscoplastic pavement).

It should be strongly emphasized that these results must be viewed with some caution as they are based on insufficient laboratory tests.

Moreover, the results of the elasto-plastic rate-independent analysis may not be simply obtained basing on Eqs. (3.18) and (3.19) because if $\eta = 0$ (no viscosity) then the Eq. (3.18) is singular. The constitutive relationships for the rate-independent model can be formulated using the procedure described in [8].

5. CONCLUSIONS

The numerical studies which have been conducted demonstrate that the material model presented in the paper may be used in order to characterize asphalt pavement's dynamic behaviour in a wide range of material parameters. As it was emphasized in the previous section, the detailed analysis needs complex experimental tests to be conducted. The numerical example we presented herein shows only the applicability of the theory. Additional testing is required of the static and dynamic ranges of load rates, in order to evaluate plastic and viscous properties of the material. For example, a somewhat similar material model presented by GONZÁLES *et al.* [7] was calibrated basing on direct tensile test results carried out for various strain rates. In our case such an experiment should be completed

by testing the material in pure shear stress state because of the complexity of the yield surface.

There exist many possible enhancements to the current model. For instance, in the case of large pressure-stress states, the material obeying the Mises–Schleicher yield condition does not exhibit the plasticity phenomenon, what leads to inadequate prediction of inelastic volume changes. Thus, some modification of the yield function leading to so-called cap models should be also considered [12]. This problems is now being studied by the author.

References

1. ABAQUS Analysis User's Manual, Ver. 6.5, 2004.
2. S. F. Brown, *Achievements and challenges in asphalt pavement engineering*, Proc. of 8th Int. Conf. on Asphalt Pavements, Seattle 1997.
3. M. A. Crisfield, *Non-linear finite element analysis of solids and structures*, Essentials and Advanced Topics, **1**–**22**, Wiley, Chichester 1991.
4. N. D. Cristescu, *Dynamic Plasticity*, World Scientific Publ., New York 2007.
5. W. Derski, R. Izbicki, I. Kisiel, Z. Mróz, *Rock and Soil Mechanics*, PWN, Warsaw 1988.
6. G. Duvaut, J. L. Lions, *Inequalities in Mechanics and Physics* [in French], DUNOD, Paris 1972.
7. J. M. Gonzáles, J. Miquel, S. H. Oller, R. Miró, *A viscoplastic constitutive model with strain rate variables for asphalt mixtures' numerical simulation*, Comp. Materials Science, **38**, 543–560, 2007.
8. W. Grzesikiewicz, W. Wojewódzki, A. Zbiciak, *Non-smooth dynamic problem formulation for elastic-perfectly plastic solid*, Theoretical Foundations of Civil Engng., **11**, 339–350, 2003.
9. M. N. S. Hadi, B. C. Bodhinayake, *Non-linear finite element of flexible pavements*, Advances in Engng. Software, **34**, 657–662, 2003.
10. J. Judycki, *Rheological models of asphalt pavement* [in Polish], Trans. of Gdańsk Univ. of Technology, **368**, 123–145, Gdańsk 1984.
11. A. S. Khan, S. Huang, *Continuum Theory of Plasticity*, Wiley, New York 1995.
12. V. A. Lubarda, *Elastoplasticity Theory*, CRC, Boca Raton 2002.
13. P. Nita, *Construction and maintenance of aircraft pavements* [in Polish], Publ. House on Transport and Telecommunications, Warsaw 1999.
14. P. Nita, *Concrete aircraft pavements. Theory and construction* [in Polish], Publ. House of the Air Force Technical Institute, Warsaw 2005.
15. P. D. Panagiotopoulos, *Inequality problems in mechanics and applications. Convex and nonconvex energy functions*, Birkhäuser, 1985.
16. P. Perzyna, *Theory of Viscoplasticity* [in Polish], PWN, Warsaw 1966.

17. J. Piłat, P. Radziszewski, *Asphalt Pavements* [in Polish], Publ. House on Transport and Telecommunications, Warsaw 2003.

18. J. C. Simo, T. J. R. Hughes, *Computational Inelasticity*, Springer-Verlag, New York 1998.

19. A. Szydło, P. Mackiewicz, *Asphalt mixes deformation sensitivity to change in rheological parameters*, J. of Materials in Civil Engng., 1–9, Jan/Feb 2005.

20. A. Zbiciak, W. Wojewódzki, *Numerical simulation of creep behaviour of asphalt pavement*, Theoretical Foundations of Civil Engng., **14**, 459–46, Warsaw 2006.

Received February 27, 2008; revised version September 4, 2008.